Formation of MEMS nanocomposit layers and investigation of their mechanical properties

S. Ponelytė*, I. Prosyčevas**, A. Guobienė***, R. Balčiūnas****, J. Puišo*****

*Kaunas University of Technology, K. Donelaičio g. 73, 44029 Kaunas, Lithuania, E-mail: sigita.ponelyte@stud.ktu.lt
**Kaunas University of Technology, Institute of Physical Electronics, Savanorių 271, 50131 Kaunas, Lithuania, E-mail: igoris.prosycevas@ktu.lt
***Kaunas University of Technology, Institute of Physical Electronics, Savanorių 271, 50131 Kaunas, Lithuania
***Kaunas University of Technology, K. Donelaičio g. 73, 44029 Kaunas, Lithuania, E-mail: asta.guobiene@ktu.lt
****Kaunas University of Technology, K. Donelaičio g. 73, 44029 Kaunas, Lithuania, E-mail: rokas.balciunas@ktu.lt
*****Kaunas University of Technology, K. Donelaičio g. 73, 44029 Kaunas, Lithuania, E-mail: judita.puiso@ktu.lt

1. Introduction

The need for effective miniaturized sensors has driven a massive research effort, with systems varying in both principal of operation, optical properties and morphology. However, despite recent advances in the field of microelectromechanical systems (MEMS) based sensors, the fabrication of miniaturized optical biosensors still tends to be a relatively difficult process, limited largely by complicated device fabrication and packaging. Integrated optical biosensors are microfabricated devices able to provide sensitive label-free biochemical detection based on the change of refractive index caused by adsorption of biomolecules, mainly used in [1]: interferometers; resonators; surface plasmon resonance and coupling-based devices.

Performance of such optical sensors depends on their surface morphology, optical and mechanical properties. Pure mechanical properties limit its use in advanced MEMS devices, shorten sensors' durability and hardness, and reduce its sensitivity. Such modification of nanocomposit materials is of considerable significance from a material science and engineering point of view.

The majority of nanocomposit materials integrated into MEMS products in recent years have been largely comprised of polymer based nanocomposites [2]. When certain properties of polymeric materials are compared to those of metals and ceramics, it becomes clear why polymers are implemented to do a job where one of the other classes of materials would previously have been used. Polymers are relatively cheaper to process and manufacture, recycle easily, are more lightweight and resistant to corrosion and can be rapidly fabricated into complex parts with little effort. It was found that water soluble silver (*Ag*) nanoparticles/polymer (poly (N-vinyl pyrrolidone) (*PVP*)) composites possess bioactive properties to suppress bacteria's growth [3]. Such *Ag/PVP* nanocomposites may be produced by heating [4, 5], photoreduction [6] and radiolysis [7, 8]. As a UV sensitive polymer, *PVP* can be easily patterned in micrometer dimension by selection of the irradiation spectrum [9]. A number of organic materials are known as protective agents for preventing silver particle coalescence, but *PVP* exhibits the best protecting properties [6, 7]. These benefits have drawn considerable attention from industry and have led to the development of strong MEMS products that can withstand the rigors of consumption.

In these researches, MEMS nanocomposit layers were formed from *PVP* and *Ag/PVP* thin films with plasmonic properties by spin-coating and photoreduction. By hot embossing procedure a diffraction grating was embossed on formed nanocomposit layer of the sensor. The effect of UV exposure time on nanocomposit films, morphology and their mechanical properties were investigated.

2. Methodology

MEMS nanocomposit thin waveguide film is deposited on the glass substrate and then a diffraction grating is embossed on it by hot-embossing procedure. A monomode waveguide is used as the primary resonant structure. It is composed of a very thin, high-refractive index layer on a transparent support. Light can be guided inside this layer through total internal reflection, as is done in optical fibers for telecommunication. The phase velocity of the guided light, characterized by the propagation constant, depends on the surrounding media [1, 10]. A change in optical properties of the latter therefore translates into a change of the propagation constant. The grating is used to probe the propagation constant. It consists of a periodic variation of waveguide thickness or refractive index [10, 11]. This periodic structure allows one to couple light waves into or out of the waveguide at the resonance condition.

2.1. Materials

Silver nitrate (*AgNO₃* analytical reagent), poly (N-vinyl pyrrolidone) (*PVP*) (average $MW = 10\,000$) and sodium dodecyl sulfate (*SDS*) ($MW = 288.38$) were obtained from Sigma Aldrich. Deionized water was prepared with a Milipore water purification system.

2.2. Preparation of silver colloid

Solution for formation of MEMS nanocomposit layers was prepared from 20% *PVP* solution (obtained by mixing 1-3 g of *PVP* with 4-6 ml of deionized water) adding to it 4-6 drops of 10% *OS* 20 (*SDS*) and shaking. After, silver nitrate (200 mg) was introduced in 20% *PVP* solution.

2.3. Formation of *PVP* and *Ag/PVP* nanocomposit layers

PVP and *Ag/PVP* films were produced on the pretreated silicon and silica substrates by spin-coating procedure. These substrates were pretreated sonically in acetone and chemically etched in the worm special chrome solution

($K_2CrO_7 + H_2SO_4 + H_2O$) for 10-12 min, and dried in air stream. Prepared solutions were spin-coated with "DYNAPERT PRECIMA" centrifuge. The spin speed was above 1800 rpm and spinning time was 30 s. The *Ag/PVP* films were dried in an oven (100ºC) for 10-12 min. Irradiation of *Ag/PVP* films were done by UV light source (Hibridas Exposure Unit MA4, power 1200 W, wavelength 300-400 nm, and exposure time from 15 s to 5 min).

2.4. Formation of diffraction grating on nanocomposit layer

Diffraction grating on formed nanocomposit layers in MEMS may be fabricated by low-cost and high-throughput replication technology such as hot embossing process. This process provides the simultaneous and single-step formation of grating on various microstructures with high accuracy. It has therefore been considered as an innovative method for a low-cost mass production of polymer microelectromechanical system (MEMS) and microoptoelectromechanical system (MOEMS) devices. Hot embossing technique is described below in Fig. 1.
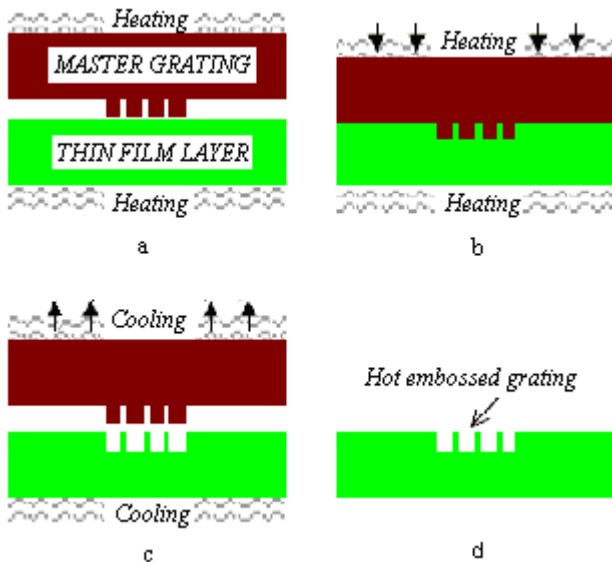

Fig. 1 Hot embossing process for diffraction grating: a – master grating and thin film placed together in furnace; b – master grating pressed into thin film; c – separating master grating and thin film; d – diffraction grating

Thin film layer and master grating (properties listed in Table 1) are placed together and fixed in the metallic mandrel between plates, tightened and put in the furnace of 120ºC (Fig. 1, a). Master grating is pressed into a thin film layer (Fig. 1, b), after adequate holding time, sensors' microchip is cooled down below its glass transition temperature and then the master grating is lifted up (Fig. 1, c). Well-defined diffraction gratings are obtained (Fig. 1, d).

Table 1

Properties of master grating

Grating periodicity	Depth, nm	400
	Periodicity, μm	4.4
Grating dimensions	Length, mm	2
	Width, mm	16
Grating lines	Parallel to the short edge	

Hot embossing procedure in polymer was analyzed in previous science researches [12].

2.5. Characterization of MEMS nanocomposit layers

The formation of MEMS functional layers were confirmed recording absorbance by SPECORD UV/VIS spectrometer. Mechanical properties were investigated using custom-made scratch testing apparatus. And morphology of microchip nanocomposit layers was investigated using Atomic Force Microscope NT-206 (AFM).

3. Results and discussions

Regardless of the material, whether metal, polymer or ceramic, the materials that make up the products must be tested under many conditions to show that they meet the requirements of the application in order to provide consumers with reliable products.

During experimental process of formation of MEMS functional layers, it was determined that performing different UV radiation time makes effect on absorbance of formed thin film layers. This evolves further analysis in determination of precise time limit for radiating samples with UV light in further design steps. For these researches, different UV lamp irradiation time was applied after formation of nanocomposit layers by spin-coating procedure. The absorbance of *Ag/PVP* layers versus irradiation time is presented in Fig. 2.
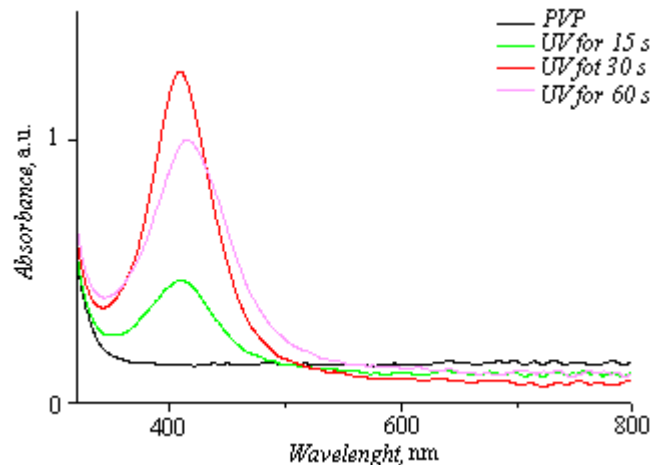

Fig. 2 Absorbance spectra of *Ag/PVP* films on glass substrate from silver colloid 200 mg *AgNO₃*

Introduction of silver nitrate in *PVP* solution affect optical properties of formed layer, i. e. wide range of silver nanoparticles give a plasmonic peak and make an effect on thin film refractive index. Fig. 2 shows how different UV radiation time gives variation in absorbance peak: narrow and sharp plasmonic peak depicts better optical properties. For *PVP* thin films a plasmon resonance is not observed. When *Ag/PVP* layer is radiated with UV light for 15 s, it gives a plasmonic peak at wavelength of 410 nm with absorbance of 0.469 a.u.. A plasmonic peak, when radiated Ag/PVP for 30 s is observed at wavelength of 408 nm with absorbance of 1.256 a.u.. After UV radiation for 60 s a plasmonic peak is observed at wavelength of 414 nm with absorbance of 0.998 a.u.. Results show that optimal UV radiation time is 30 s, i. e. too long radiation time decreases absorbance of nanocomposit layer.

The scratch test has been gaining more and more credibility in polymer applications as research has continued over the years. When addressing scratch resistance, there are two main areas of focus: aesthetics and protection. The former is important to applications such as paint, gloss-coats or surfaces that will be devalued by blemishes, scuffs, mars or gouges. The latter is relatively self-explanatory in that the surface must be kept free of scratches than can damage either delicate parts on the surface, like a microchip, or the surface beneath a coating. The concept of custom-made scratch testing apparatus (Fig. 3) is to draw an indenter through the sample with the increasing load and register tangential and normal feedback. Afterwards sample is examined under an optical microscope in search of characteristic defects.
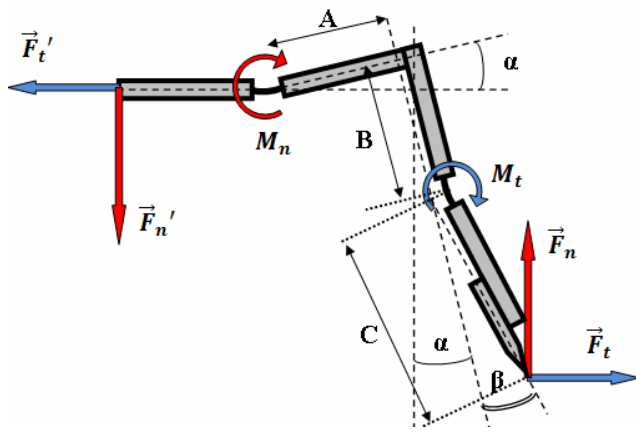

Fig. 3 Custom-made apparatus for scratch test

In custom-made apparatus, A, B and C are cantilevers, where $A = 51.5$ mm, $B = 49.5$ mm and $C = 58$ mm. Mass of the weight used for scratch is $m = 7.765$ g. The scratch hardness is analogous to the indentation hardness given by Briscoe [13], as the normal load F_n divided by the contact area, which for a spherical indenter is the area of a circle with the diameter equal to the width of the scratch track d

$$H_s = q\,\frac{4F_n}{\pi d^2} \tag{1}$$

here F_n is normal load. An additional parameter q was adopted for polymer scratch behavior. q is a parameter that corresponds to the recoverability of the polymer. If full recovery is assumed, q is taken to be equal to 1 [14-15].

Scratch tests were performed for two different MEMS nanocomposit layers: *PVP* and *Ag/PVP* nanocomposit thin films. The obtained scratch diagrams of Force versus Displacement are presented in Fig. 4. Scratch diagram of sensors' layer formed from 20% *PVP* is given in Fig.4, a. Its delaminated region is given in Fig. 4, b. The width of the scratch track is ~25 μm. Pileups are observer. Scratch diagram for *Ag/PVP* nanocomposite layer is presented in Fig. 4, c, and its delaminated region is shown in Fig. 4, d. The width of the scratch track is ~30 μm. A clean delamination with no pileups is observed.

a

b

c
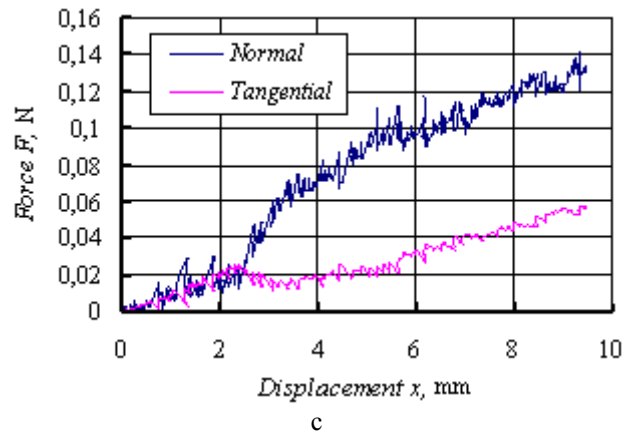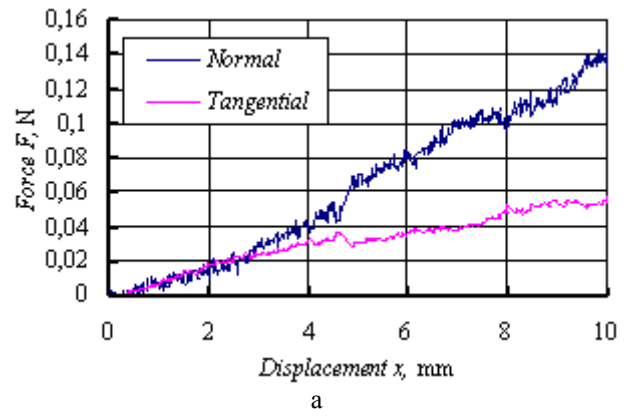
d

Fig. 4 Scratch tests and scratch views of *PVP* and *Ag/PVP* nanocomposites on silicon substrate: a – 20% *PVP*; b – scratch view of 20% *PVP*; c – 200 mg *Ag-NO₃*/20% *PVP*; d – scratch view 200 mg *Ag-NO₃*/20% *PVP*

In a scratch test, surface friction behavior as well as visibility can be characterized by applying controlled scratches to the surface of materials. This is shown in friction diagrams (coefficient of friction versus displacement). For *PVP* layer (Fig. 5, a) the coefficient of friction steadily increases and then drops dramatically to the constant average of 0.43. These two regions depict groove formation and coating delamination areas. Fig. 5, b shows how the coefficient of friction drops down to ~0.25 and then increases steadily up to ~0.43, i.e. coating delamination occurs at low normal load (~0.019 N).
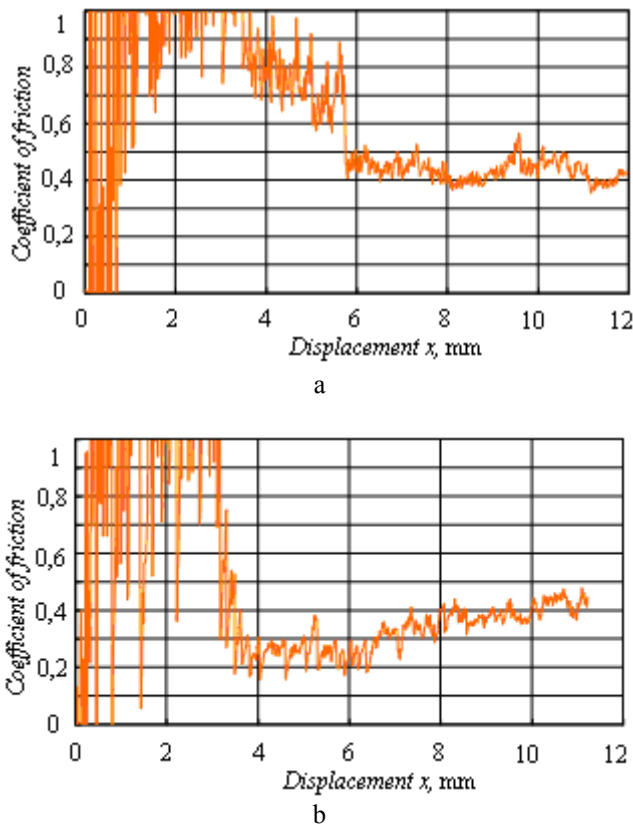
Fig. 5 Friction diagrams of *PVP* and *Ag/PVP* nanocomposites on silicon substrate: a – 20% *PVP*; b – 200 mg *AgNO₃*/20% *PVP*

From the obtained experimental data of scratch testing hardness of each formed layer is evaluated: the width of the scratch track made in *PVP* layer is $d = (11.30 \pm 0.44)$ μm, the corresponding normal load is $F_n = (0.028 \pm 0.009)$ N. Thus from the formula (1), hardness is $H = (239 \pm 74)$ MPa for layers formed from 20% *PVP*. For sensor microchip with *Ag/PVP* nanocomposit layer: the width of the scratch track is $d = (8.61 \pm 0.44)$ μm, the corresponding normal load is $F_n = (0.019 \pm 0.009)$ N, thus hardness is $H = (321 \pm 158)$ MPa.

Using ellipsometer thickness of *PVP* and *Ag/PVP* thin layers formed on *Si* plate were measured, and only approximate results obtained: thickness range of both layers were 0.5 ± 0.1 μm. In order to get more precise information about thin films, there was used Atomic Force Microscope NT–206 for analysis of surface morphology. Characteristics of noncontact silicon cantilever NSC11/15, used for measurements are given in Table 2.

Table 2
Characteristics of noncontact silicon cantilever

Length $l \pm 5$, μm	Width $w \pm 3$, μm	Thickness, μm	Resonant frequency, kHz	Force constant, N/m
200	40	2.0	65	3.0

In AFM a flexure positioning system is integrated, seeking to ensure the wide diapason of positioning and real nanometric accuracy of 2 nm [16]. Following results were obtained: thickness of *PVP* layer is $d_z = 474 \pm 2$ nm and thickness of *Ag/PVP* layer is $d_z = 542 \pm 2$ nm. Morphology of such MEMS nanocomposit layers formed

on silicon plate is presented in Fig. 6. According AFM measurements results, the roughness (R_q is the standard deviation of the *Z* values within a given area) of surfaces presented in Fig. 6, a, b was 15.3 nm for *PVP* and 9.6 nm for *Ag/PVP*. This implies that *Ag/PVP* and *PVP* surfaces are very smooth with nano-size irregularities.
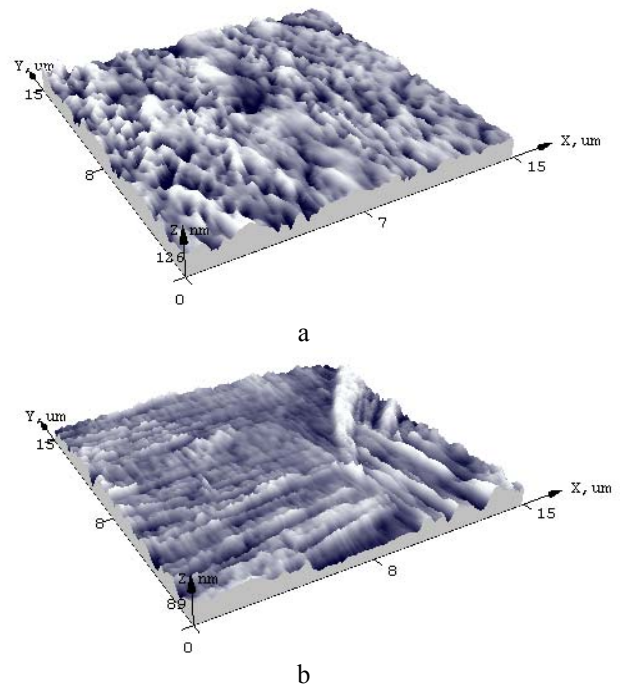

Fig. 6 AFM images of *PVP* and *Ag/PVP* nanocomposites on silicon substrate: a – 20%*PVP*; b – 200 mg *AgNO₃*/20% *PVP*

The adhesion properties of *PVP* and *Ag/PVP* nanocomposites are in Fig. 7. Deflection force curves with large hysteresis between loading and unloading parts, due to their elastoplastic nature are observed in typical polymeric materials [17]. The maximum load of *PVP* is 55 nN, for *Ag/PVP* layers we need 94 nN. It is also found that *PVP* films required adhesive force of 23 nN to approach the surface with a probe. We suppose that the silver nanoparticles in *PVP* matrices produced harder and flatter layer compared with pure *PVP* layers [18].
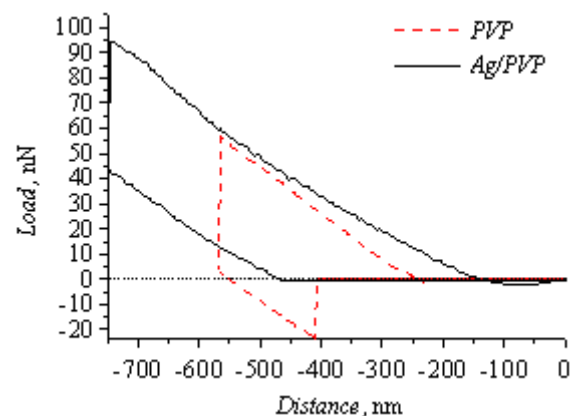

Fig. 7 Force curves of *PVP* and *Ag/PVP* nanocomposites

Analyses of optical and mechanical properties, and surface morphology prove the relevance of formed

microchip *Ag/PVP* nanocomposit layer and show how surface parameters and hardness of thin films changes when silver nanoparticles are introduced. These conclusions enable further design process of diffraction grating formation using 200 mg *AgNO₃*/20% *PVP*, coated on glass substrate.
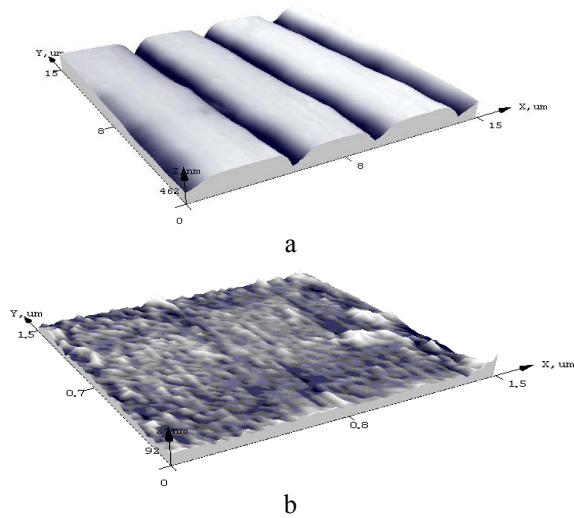

Fig. 8 Diffraction grating formed on nanocomposite layer:
a – diffraction grating; b – grating ridge

Using hot-embossing technological procedure (Fig. 2) a diffraction grating was imprinted on formed nanocomposit layer. Results, obtained after investigation of surface morphology using AFM, show that a designed sensors' microchip with embossed diffraction grating (Fig. 8, a) in it has a very smooth surface (roughness $R_q = 6.3$ nm) (Fig. 8, b) with diffraction grating properties of average grating height of 333 nm, and width of 4.4 μm.

4. Conclusions

1. The dependence of the shape, size, optical and mechanical properties of *PVP* and *Ag/PVP* nanocomposit layers in MEMS on UV irradiation time and silver salts concentration were investigated by UV-VIS spectroscopy, custom made scratch test apparatus and AFM. Plasmonic resonance phenomenon is observed in nanocomposit Ag/*PVP* layer at wavelength of 408 nm with absorbance of 1.256 a.u.

2. Large errors of hardness values are influenced by the large relative errors of normal load – the scratch apparatus lacked sensitivity. It was not possible to acquire true values of hardness for *PVP*, however, referring to other work about polymer scratch testing it is possible to assume that the hardness for polymers is around 50MPa [13]. This great mismatch can be influenced by the low thickness of the coating (around 7% of the width of the scratch track).

3. However, MEMS with *Ag/PVP* nanocomposit layer is harder than the one without *PVP*. This fact also influenced the clean delamination of this layer during the scratch test. From results obtained using custom-made apparatus for scratch test and atomic force microscope, formed *Ag/PVP* layer is harder and flatter compared to *PVP* layer, i.e. hardness of *PVP* is 239 ± 74 MPa, and for *Ag/PVP* nanocomposit layer hardness was 321 ± 158 MPa.

4. Using a hot – embossing procedure, parameters of imprinted diffraction grating on nanocomposite layer were similar to parameters of master grating. This proves effectiveness of used technological process for formation of diffraction grating.

5. These investigations are based on MEMS researches in driving the ever-accelerating race to construct smaller, faster, cheaper and more efficient optical sensor device, successfully integrated in electronic and biological systems such as in Optical Waveguide Lightmode Spectroscopy.

References

1. **Lambeck, P.V.** Integrated optical sensors for the chemical domain. -Meas. Sci. Technol., 2006, 17, p.93-116.
2. **Bertrand-Lambotte, P., Loubet, J.L., Verpy, C., Pavan, S.** Nano-indentation, scratching and atomic force microscopy for evaluating the mar resistance of automotive clearcoats: study of the ductile scratches. -Journal of Thin Solid Films, 2001, 398, p.306-312.
3. **Surova, E.,I., Klechkovskaya, V.V., Kopeikin, V.K., Buffat, P.A.** Stability of Ag nanoparticles dispersed in amphiphilic organic matrix. -Journal of Crystal Growth, 2005, 275, p.e2351-e2356.
4. **Kim, J.S.** Antibacterial activity of Ag^+ ion-containing silver nanoparticles prepared using the alcohol reduction method. -Journal of Industrial and Engineering Chemistry, 2007, 13, p.718-722.
5. **Jin, M., Zhan, X., Nishimoto, S., Liu, Z., Tryk, D. A., Murakami, T., Fujishima, A.** Large-scale fabrication of Ag nanoparticles in PVP nanofibres and net-like silver nanofibre films by electrospinning.-Nanotechnology, 2007, 18, p.1-7.
6. **Xu, G.N., Qiao, X.L., Qiu, X.L., Chen, J.G.** Preparation and characterization of stable monodisperse silver nanoparticles via photoreduction. -Colloids and Surfaces: Physicochemical and Engineering Aspects, 2008, 320, p.222-226.
7. **Kang, Y.O., Choi, S.H., Gopalan, A., Lee, K.P., Kang, H.D., Song, Y.S.** Tunning morphology of Ag nanoparticles in the Ag/polyaniline nanocomposites prepared by [gamma]-ray irradiation. -Journal of Non-Crystalline Solids, 2006, 352, p.463-468.
8. **Yu, D., Sun, X., Bian, J., Tong, Z., Qian, Y.** Gamma-radiation synthesis, characterization and nonlinear optical properties in suspensions. -Physica E: Low-dimensional Systems and Nanostructures, 2004, p.50-55.
9. **Li, Z., Li, Y., Gian, X.F., Yin, J., Zhu, Z.K.** A simple method for selective immobilization of silver nanoparticles. -Appl. Surf. Sci., 2005, 250, p.109-116.
10. **Vörös, J., Ramsden, J. J., Csúcs, G., Szendro, I., Paul, S.M., Textor, M., Spencer, N.D.** Optical grating coupler biosensors. -Biomaterials, 2002, v.23, issue 17, p.3699-3710.
11. **Grieshaber, D., MacKenzie, R., Voros, J., Reimhult, E.** Electrochemical Biosensors - Sensor Principles and

Architectures. -Sensors, 2008, 8, p.1400-1458.

12. **Guobienė, A.** Formation and analysis of periodic structures in polymer materials. -Doctoral dissertation. -Kaunas: Technologija, 2005.-86p.

13. **Briscoe, B.J., Evans, P.D., Pelillo, E., Sinha, S.K.** Scratching maps for polymers. -Wear, 1996, 200, p.137-147.

14. **Zabulionis, D., Gailius, A.** Numerical modeling of creep functions of laminated composites. -Mechanika. -Kaunas: Technologija, 2007, No.3(65), p.5-11.

15. **Browning, R L.** Quantitative characterization of polymer scratch behavior using a standardized scratch test. -Thesis at Texas A&M University, 2006.-85p.

16. **Lendraitis, V., Mizarienė, V., Seniūnas, G.** Nanopositioning – methods and means. -Mechanika. -Kaunas: Technologija, 2007, No.2(64), p.49-54.

17. **Reynaud, C., Sommer, F., Quit, C., Bounia, N.El, Duc, T.M.** Quantitative determination of Young's modulus on biphase polymer system suing atomic force microscopy. -Surf. Interface Anal., 2000, 30, p.185-189.

18. **Santner, E., Stegemann, E.** Adhesion measurements by AFM – a gateway to the basics of friction. -Proc. of the Meeting of the International Research Group on Wear of Engineering Materials (IRG-WOEM OECD), Uppsala, 2005, p.10.

S. Ponelytė, I. Prosyčevas, A. Guobienė, R. Balčiūnas, J. Puišo

MIKROELEKTROMECHANINIŲ SISTEMŲ SU NANOKOMPOZICINIAIS SLUOKSNIAIS FORMAVIMAS IR JŲ MECHANINIŲ SAVYBIŲ TYRIMAS

R e z i u m ė

Straipsnyje pateiktas nanokompozicinių sluoksnių, plačiai naudojamų įvairiose mikroelektromechaninėse sistemose (MEMS), formavimas ir jų mechaninių bei morfologinių savybių tyrimas. Nanokompoziciniai sluoksniai formuojami ant kvarcinio stiklo ir silicio plokštelių centrifugavimo būdu nusodinant susintetintą *PVP* arba *Ag/PVP* tirpalą. Suformuotas sluoksnis apšvitinamas UV lempa. Remiantis SPECORD UV/VIS spektrometru gautais rezultatais, buvo nustatyta, kad nuo apšvitinimo trukmės priklauso nanokompozicinių sluoksnių absorbcijos savybės. Įbrėžimo matavimais buvo ištirtos ir palygintos atskirų sluoksnių (*PVP* ir *Ag/PVP*) mechaninės savybės, t. y. trinties koeficiento priklausomybė nuo poslinkio. Suformuotų MEMS nanokompozicinių sluoksnių elastinės savybės ir morfologija buvo ištirtos naudojantis atominių jėgų mikroskopu NT-206.

S. Ponelytė, I. Prosyčevas, A. Guobienė, R. Balčiūnas, J. Puišo

FORMATION OF MEMS NANOCOMPOSIT LAYERS AND INVESTIGATION OF THEIR MECHANICAL PROPERTIES

S u m m a r y

This paper presents formation and investigation of morphology and mechanical properties of nanocomposit layers, widely used in microelectromechanical systems (MEMS). These nanocomposit layers were fabricated on silicon and silica substrates using spin coating procedure from synthesized *PVP* or *Ag/PVP* solutions. After spin coating the formed MEMS layer is irradiated with UV light. As later results of investigation using SPECORD UV/VIS spectrometer showed, an irradiation time leads to different absorbance properties of nanocomposit layers. Mechanical properties of both (*PVP* and *Ag/PVP*) layers were investigated using a scratch test, i.e. the hardness of each formed layer were evaluated. Elastic properties and morphology were investigated using Atomic Force Microscope NT-206.

С. Понелите, И. Просычев, А. Гуобене, Р. Бальчунас, Ю. Пуйшо

НАНОКОМПОЗИТНЫЕ СЛОИ ДЛЯ МИКРОЭЛЕКТРОМЕХАНИЧЕСКИХ СИСТЕМ И ИХ МЕХАНИЧЕСКИЕ СВОЙСТВА

Р е з ю м е

В статье рассматривается способ формирования нанокомпозитных слоев, приводится результаты исследования морфологии и механических свойств этих слоев, которые используются в микроэлектромеханических системах (MEMS). Слои были изготовлены на кремниевых подложках путем центробежного нанесения растворов полимеров *ПВП* и *Ag/ПВП*. После сушки покрытия и облучения УФ светом сформирован нанокомпозитный слой. Оптические свойства были исследованы с использованием UV-VIS SPECORD спектрометра и показали, что, в зависимости от времени облучения, меняется оптическая плотность слоев. Механические свойства обоих (*ПВП* и *Ag/ПВП*) слоев были исследованы с помощью скретч теста. Упругие свойства и морфология исследовались с помощью атомно-силового микроскопа NT-206.